Protein Dynamics of Glycogen Phosphorylase†

Steven M. Martin, John R. Lindroth, and John W. Ledbetter*
Department of Biochemistry, Medical University of South Carolina, Charleston, South Carolina 29425
Received March 4, 1986; Revised Manuscript Received May 14, 1986

ABSTRACT: The glycogen phosphorylase molecule absorbs the ultraviolet energy of a nitrogen laser to form an excited state of the cofactor. The decay rate of this state has a lifetime of 6.7 μs, and its sensitivity to bound substrates presents a new perspective of the mechanism. A careful analysis of the decay curve for native enzyme and cofactor analogues showed that the lifetime depends on the conformation of protein groups at the active site and how the residues change with bound substrate. The reactive ternary complexes obtained from either direction of the reaction yielded the same lifetime, indicating a change in the active-site conformation to a common configuration for the cofactor and substrate phosphate. This configuration indicates an increase in the cofactor 5′-PO_4 pK_a and a possible proton shuttle. The pyridoxal 5′-pyrophosphate reconstituted enzyme showed no conformational change alone or in the presence of oligosaccharide. This result does not support an electrophilic attack by the 5′-PO_4 phosphorus.

The glycogen phosphorylase molecule provides us with a formidable challenge in understanding its dynamic structure during catalysis. The X-ray analyses by Sygusch et al. (1977) and Weber et al. (1978) and later refinements have provided invaluable insights into the molecular structure of the molecule. However, with the conformational changes within the molecule in changing to the R state, obtaining a concept of dynamic events has been difficult. The X-ray data of bound glucose 1-phosphate (glucose-1-P) (Johnson et al., 1980), glucose cyclic 1,2-phosphate (glucose-1,2-P) (Withers et al., 1982), and heptulose 2-phosphate (heptulose-2-P) (McLaughlin et al., 1984) have suggested a causative relationship between the phosphates of the vitamin B_6 cofactor and substrates. The glucosyl transfer from pyridoxal pyrophosphate glucose (Withers et al., 1981a; Takagi et al., 1982) seems to provide evidence that a chemical interaction between phosphates exists.

The ^{31}P nuclear magnetic resonance (NMR)[1] results have also shown that the cofactor phosphate exhibits a change on the binding of substrates. From their results, Klein et al. (1982) proposed that the phosphate acts as a participant in a proton shuttle in which the protonation of 5′-phosphate promotes the oxygen bond cleavage of glucose-1-P. Withers et al. (1981b) interpreted the NMR spectra otherwise and proposed an electrophilic attack by a constrained dianion of the 5′-phosphate group. Johnson et al. (1980) proposed a nucleophilic attack by the 5′-phosphate of the C1 carbon of glucose-1-P. This attack required a conformational change of the substrate from that structure shown in the X-ray analysis.

Cornish and Ledbetter (1984a) observed that the cofactor of phosphorylase absorbs energy of the nitrogen laser. The energy populates a well-known singlet state whose first-order decay has a lifetime of a few microseconds. Quite interestingly, the lifetime depended on specific substrate binding. Exhaustive experiments with far more precise instrumentation have now reproduced the results and allowed a more thorough analysis of data obtained with both phosphorylases *a* and *b* and three cofactor analogues. The new data show changing protein conformations that affect the environment about the cofactor. The data demonstrate, through the binding of ligands from either direction of the reaction, a common active ternary complex showing protein charge movement away from the cofactor. Decay rates of the pyridoxal 5′-pyrophosphate reconstituted enzyme do not demonstrate conformations of the active ternary complex. Consequently, the data do not support an electrophilic role for the phosphorus of 5′-PO_4 in the catalysis.

Experimental Procedures

The enol structure of the pyridoxal-P cofactor of glycogen phosphorylase absorbs well the 337-nm emission of the nitrogen laser. When excited, the cofactor exhibits a transient absorption at about 470 nm (Walters et al., 1982; Cornish & Ledbetter, 1984a). Cornish and Ledbetter (1984a) describe the absorption decay as the sum of two exponentials: a strong first-order decay with a rate constant of 1.52×10^5 s^{-1} and a weak slowly decaying tail with a rate constant of 5.74×10^3 s^{-1}. The source of the strong fast decay is an excited singlet state with the 3-OH proton of pyridoxal on the imine nitrogen of the Schiff base linkage. The initial proton transfer takes place in the first excited singlet state where the 3-OH becomes 10^7 times more acidic (Ledbetter et al., 1979). After proton transfer and fluorescence with a large Stokes shift, the transfer back to the proton requires microseconds. This lower state with the proton still on the imine nitrogen exhibits the absorption at 470 nm.

Walters et al. (1982) and Cornish and Ledbetter (1984a) describe details on the method of observation of the transient absorption and decay. A 10-ns ultraviolet pulse of a nitrogen laser operated at 1.4 Hz excites the enzyme sample in a small cuvette. At 90° to this excitation, the 476.5-nm beam from an Ar^+ laser probes the sample. A shutter pulses the Ar^+ laser beam for 15 ms during which time the electronics fire the nitrogen laser. The Ar^+ laser output was 60 mW which before probing the sample an attenuator reduced to 1–2 mW. An RCA 4526 tube with a 200 Ω load resistance detected the light intensity. The 7A16A vertical amplifier of a Tektronix 7912AD programmable digitizer recorded the voltage sweep. Each sweep contained the maximum 512 digitized points. An

† This work was partially supported by U.S. Department of Health and Human Services Grant GM33409.

[1] Abbreviations: NMR, nuclear magnetic resonance; AMP, adenosine 5′-monophosphate; EDTA, ethylenediaminetetraacetic acid; G1P, glucose 1-phosphate (α-D-glucopyranose 1-phosphate); G12P, glucose cyclic 1,2-phosphate (α-D-glucopyranose cyclic 1,2-phosphate); DTT, dithiothreitol; Tris, tris(hydroxymethyl)aminomethane; PLP, pyridoxal 5′-phosphate; PL, pyridoxal.

0006-2960/86/0425-6070$01.50/0

IBM PC/AT computer controlled the digitizer and collected the data averaged over 64 pulses. An IMSL Inc. nonlinear least-squares regression subroutine based on the Levenberg–Marquardt algorithm compiled with an IBM Professional Fortran program fitted the requested number of parameters to the data. A Hewlett-Packard 7470A plotter prepared the results for publication.

Except for the substitution of DTT for cysteine, we prepared glycogen phosphorylase *b* (EC 2.4.1.1) from fresh rabbit muscle according to the method of Fischer and Krebs (1958). The activity was measured in the direction of glycogen synthesis. Passage of the enzyme through a charcoal/cellulose (1:1) column removed the AMP. From this enzyme, we prepared phosphorylase *a* with phosphorylase kinase according to the procedure of Krebs et al. (1964). The preparation of apophosphorylase *b* went according to the method of Shaltiel et al. (1966) with some exceptions. The protein remained in resolution buffer for 2 h. Passage over a Sephadex G-25 medium column (2.5 cm × 75 cm) equilibrated with 0.2 M imidazole and 0.06 M cysteine at pH 6.0 completed the resolution. Dialysis overnight at 4 °C against 0.04 M glycerophosphate and 0.03 M β-mercaptoethanol at pH 6.8 followed. Reconstitution of apophosphorylase with pyridoxal-5′-P analogues proceeded according to the method of Parrish et al. (1977).

The preparation of glucose cyclic 1,2-phosphate went according to the method of Zmudzka and Shugar (1964) and to the modification by Dreyfus et al. (1980). Wittmann (1962) described the procedure for the preparation of pyridoxal 5′-fluorophosphate using 2,4-dinitrofluorobenzene in the presence of triethylamine. Using the method of Shimomura and Fukui (1978), we prepared the Li salt of pyridoxal 5′-pyrophosphate which we then dissolved in 30:70 water/acetone and passed over a Sephadex LH-20 column (1 × 30 cm). The pyridoxal 5′-pyrophosphate was verified by thin-layer chromatography according to Shimomura and Fukui (1978). Anal. Calcd for $C_8H_9O_9NP_2{\cdot}2Li{\cdot}H_2O$: C, 26.91; H, 3.11; N, 3.92. Found: C, 26.84; H, 3.07; N, 3.63.

For the laser samples, 3× recrystallized phosphorylase was dissolved in the appropriate buffer and concentrated to about 1.0 mM in monomer. The addition of ligands occurred directly to the cell.

Results

Figure 1A shows the typical decay curve obtained for rabbit muscle glycogen phosphorylase. Compared to that of Cornish and Ledbetter (1984a), the apparatus now digitizes the decay curve with much improved resolution. A comprehensive analysis has shown a more complicated decay structure and has proven of great value in elucidating the effect of substrates on the enzyme.

The curve of Figure 1A does not follow first-order or second-order kinetics. Decay of the proton transfer band of Schiff bases in aprotic solvents is first order, but in the phosphorylase system other transient absorptions appear. Hence, we will begin as before with a nonlinear least-squares fit of the equation:

$$A = A_1e^{-k_1t} + A_2e^{-k_2t}$$

where A is the absorbance. The residual plot of Figure 1B shows that the equation did not yield a satisfactory fit. Before proceeding with other equations, consider two important aspects of this fitting procedure. First, the program will fit only the data in the time frame presented. The data in a selected sweep may not contain significant data on decays in shorter or longer time frames for a completely adequate fit.

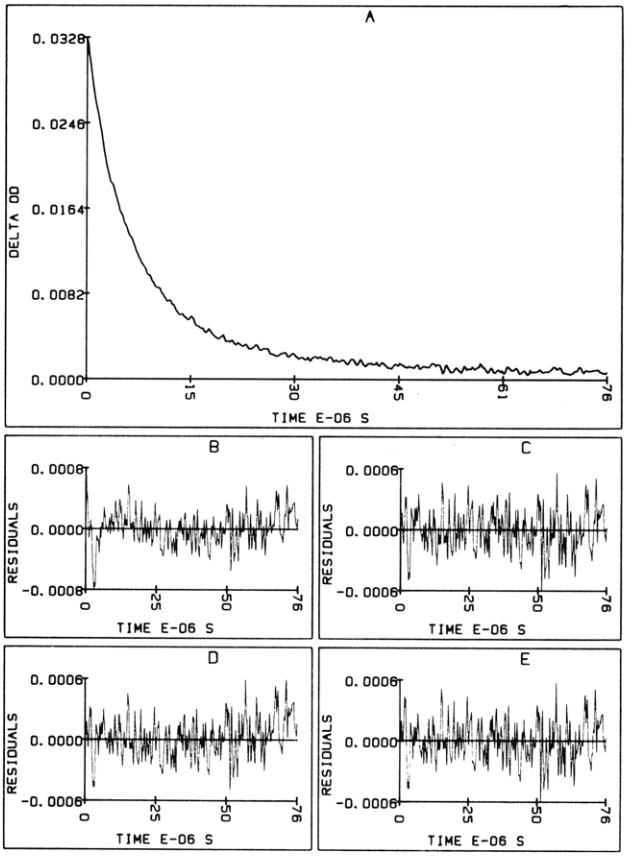

FIGURE 1: (A) Decay of absorbance at 476.5 nm for phosphorylase *b* in 2 mM dithiothreitol and 0.3 mM EDTA at pH 6.8. Sweep, 10 μs/division. (B) Residual plot of (A) with 0.027 exp(−169000*t*) + 0.0053 exp(−29500*t*). (C) Residual plot of (A) with 0.0064 exp(−408000*t*) + 0.023 exp(−132000*t*) + 0.0033 exp(−21000*t*). (D) Residual plot of (A) with 0.0027 exp(−694000*t*) + 0.025 exp(−158000*t*) + 0.005 exp(−30000*t*). (E) Residual plot of (A) with 0.0035 exp(−700000*t*) + 0.025 exp(−149000*t*) + 0.004 exp(−30000*t*) + 0.0004 exp(−6000*t*).

Second, the program fits the equations without regard to validity, and, therefore, we should constantly question the accuracy of the values of the regression. For example, fitting the above data to three exponentials, as in Figure 1C, improved the fit, but the regression values lost reliability. The correlation coefficients were too high.

The fit by two exponentials showed deviations at both fast and slow times. To observe the fast decay, we held one decay to $k = 3 \times 10^4$ s^{-1}, the slowest decay of the two-exponential fit, and fitted three exponentials, asking for two rate constants and three amplitudes. Figure 1D shows the resulting residual curve. The rate constant for the fast decay is 7×10^5 s^{-1}. Other experiments confirmed this value. Deviations which now occur in the residual curve of Figure 1D at long times indicate the presence of another decay. This long decay is the one found by Cornish and Ledbetter (1984a) and can more easily be seen at 200- and 500-μs sweeps. The data at 200 μs in Figure 2A yielded 6.8×10^3 s^{-1} for the long decay in a three-exponential fit, holding one decay to 3×10^4 s^{-1}. For the 500-μs sweep in Figure 3A, again holding only $k_2 = 3 \times 10^4$ s^{-1} constant, the decay occurred at 6×10^3 s^{-1}. The decay at 3×10^4 s^{-1} for phosphorylase *b* was weak for enzyme alone, but in the presence of glucose phosphates, as Figure 4A shows, it became much stronger.

Consequently, unlike the two-exponential treatment given previously, we now must provide for four exponentials: three of these have weak amplitudes and must be assigned to a process other than the dominant singlet-state decay repre-

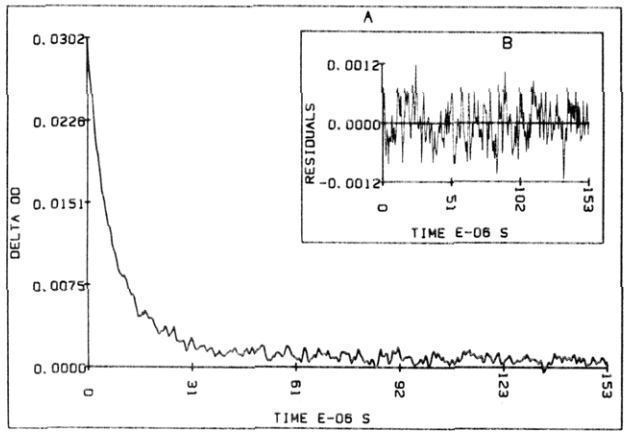

FIGURE 2: (A) Decay of absorbance at 476.5 nm for phosphorylase *b* in 2 mM dithiothreitol and 0.3 mM EDTA at pH 6.8. Sweep, 20 μs/division. (B) Residual plots of (A) with 0.026 exp(−145000*t*) + 0.0014 exp(−30000*t*) + 0.0015 exp(−6800*t*).

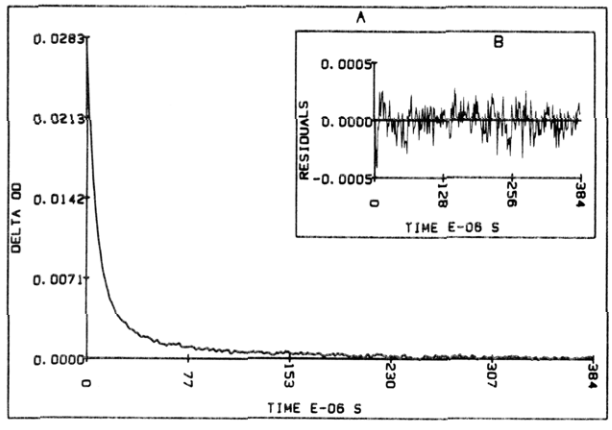

FIGURE 3: (A) Decay of absorbance at 476.5 nm for phosphorylase *b* in 2 mM dithiothreitol and 0.3 mM EDTA at pH 6.8. Sweep, 50 μs/division. (B) Residual plot of (A) with 0.023 exp(−138000*t*) + 0.004 exp(−30000*t*) + 0.0009 exp(−6000*t*).

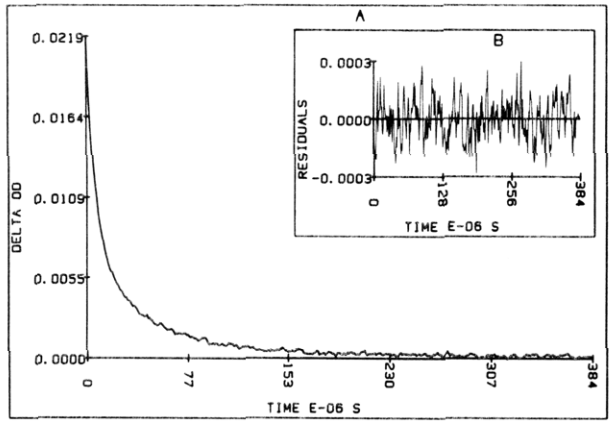

FIGURE 4: (A) Same as in Figure 3A but with 100 mM glucose cyclic 1,2-phosphate added. (B) Residual plot of (A) with 0.013 exp(−165000*t*) + 0.0075 exp(−28000*t*) + 0.0009 exp(−5000*t*).

senting the proton transfer. Therefore, to make the analyses meaningful, we held the rates of these three weak decays constant at 7×10^5, 3×10^4, and 6×10^3 s^{-1}. For a final fit, we let the amplitudes of the weak decays vary (three variables) and fitted the proton transfer decay rate, k_2, and amplitude, A_2 (two variables), for a total of five variables:

$$A = A_1e^{-7\times10^5t} + A_2e^{-k_2t} + A_3e^{-3\times10^4t} + A_4e^{-6\times10^3t}$$

Now, fitting Figure 1 with this equation yielded the residuals of Figure 1E. By avoiding the pitfalls of curve fitting, we

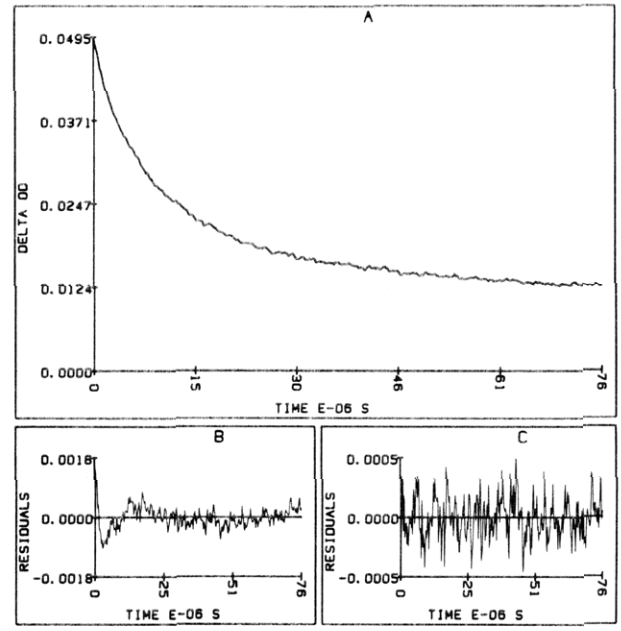

FIGURE 5: (A) Decay of absorbance at 476.5 nm for pyridoxal phosphorylase *b* in 2 mM dithiothreitol and 0.3 mM EDTA at pH 6.8. Sweep, 10 μs/division. (B) Residual plots of (A) with 0.028 exp(−118000*t*) + 0.019 exp(−6000*t*). (C) Residual plot of (A) with 0.006 exp(−522000*t*) + 0.026 exp(−93000*t*) + 0.018 exp(−4500*t*).

believe the rates of the weaker decays are realistic, and by holding them constant, we can observe the effect of substrates on the proton transfer decay. We do assume no rate change of the weaker decays, and because they are weak, the error will be minimal. For example, a doubling of k_1 leads only to an 8% change in k_2. A 2-fold change in k_3 produces a 15% change in k_2. An equivalent change in k_4 has less than a 1% effect on k_2.

Evidence exists that the three weak decays come from a triplet state. Cornish and Ledbetter (1985) recently found in water the triplet state of pyridoxal 5′-phosphate absorbing in the blue region and decaying with a rate constant of 10^6 s^{-1}, essentially the rate of the fast decay observed here. While here the Schiff base of pyridoxal 5′-phosphate is present in the enzyme, we have also seen similar behavior in free Schiff bases of amino acids and in aspartate aminotransferase (Cornish & Ledbetter, 1984b). In all these cases, the triplet-state decay is complicated by the decay of three species all absorbing in the blue. For the analysis of the effect of substrates on the decay, we have resorted to the above procedure which separates the proton decay from the triplet decay scheme. While it may seem complicated, the procedure proved worthwhile for the explanation of the substrate effects. We were also reassured that for enzyme alone the current results agree well with the previous values of 1.52×10^5 and 6.0×10^3 s^{-1} (Cornish & Ledbetter, 1984a). The most significant difference between the results presented here and those presented earlier lies in the effects of glucose-1-P, which increases the decay amplitude at 3×10^4 s^{-1}.

The same procedure proved worthwhile for the analysis of phosphorylase *a* and of pyridoxal 5′-fluorophosphate reconstituted and pyridoxal 5′-pyrophosphate reconstituted enzyme. However, the decay curve of Figure 5A for pyridoxal-reconstituted enzyme differs notably. A strong fast decay remains present, but the amplitude of the longest decay is much greater. The residual curve of Figure 5B clearly shows that two exponentials do not fit the decay and that a faster component is present. Three exponentials produced better results in the residuals of Figure 5C with low correlations for the 5

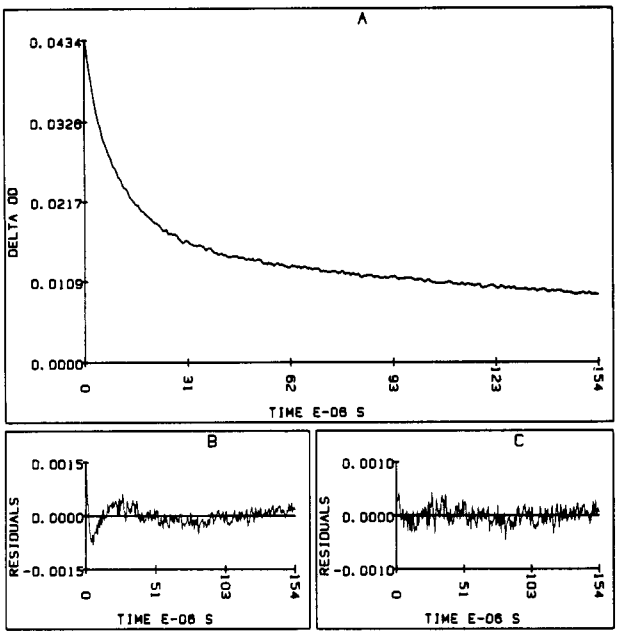

FIGURE 6: (A) Decay of absorbance at 476.5 nm for pyridoxal phosphorylase *b* in 2 mM dithiothreitol and 0.3 mM EDTA at pH 6.8. Sweep, 20 μs/division. (B) Residual plots of (A) with 0.026 exp(−99 900*t*) + 0.017 exp(−4100*t*). (C) Residual plot of (A) with 0.005 exp(−500000*t*) + 0.023 exp(−86000*t*) + 0.016 exp(−3800*t*).

$\times 10^5$ s^{-1} decay constant. This is probably a realistic number because of the 7×10^5 s^{-1} constant found for phosphorylase. The rate for the longest decay also appears reasonable by comparison. For a better determination, Figure 6A shows the decay at a 200-μs sweep. The fit of the data showed that a rate constant of 4×10^3 s^{-1} is realistic. We assign the decay at 9×10^4 s^{-1} in the fit of Figure 5C to the decay of the singlet state of the proton transfer. This good fit does not indicate the presence of a fourth exponential as found with phosphorylase *b*. The decay at 3×10^4 s^{-1} was not noted; although, as an intermediate in the triplet decay mechanism, it could still be present but not observable. The absence of the 5′-PO_4 group may allow more interaction of the solvent with the triplet state to produce rapidly the slowly decaying species.

The direction and magnitude of the change in the rate constant of the proton transfer for pyridoxal-reconstituted enzyme also appear reasonable. By comparison, in dimethylformamide, the PLP Schiff base of tris(hydroxymethyl)aminomethane (Tris) yielded a rate constant of 2.1×10^5 s^{-1} while the PL base gave 1.3×10^5 s^{-1}. This 38% decrease agrees well with the 40% change for the enzyme. Consequently, we feel that the comparisons between the two enzymes deal with the same transition decay.

The addition of substrates or inhibitors to phosphorylase *a* or *b* or to the analogue-reconstituted phosphorylase caused changes in the rate of the transient decay. Tables I and II list the rate constants associated with many ligands and their combinations. We have used this sensitivity to ligands to provide information on the mechanism of the phosphorylase reaction. Clearly, from the tables the transient rate constant is sensitive to the substrates in a reproducible manner. The binding of AMP by phosphorylase *b* also affects the rate constant of enzyme plus substrate. Table III demonstrates for P_i and for glucose-1-P that AMP is necessary for obtaining numbers equivalent to the respective ones of Table I.

Table I: Transient Decay Rate Constants for Enzymes and Substrates

substrate[a]	rate constant ($s^{-1} \times 10^{-5}$) phosphorylase *a*	phosphorylase *b*[b]
none	1.51 ± 0.02	1.49 ± 0.02
glucose	1.42 ± 0.02	1.27 ± 0.03
maltoheptaose	1.45 ± 0.03	1.49 ± 0.02
glycogen	1.45 ± 0.04	1.47 ± 0.04
P_i	1.93 ± 0.02	2.05 ± 0.03
P_i + glucose	1.48 ± 0.02	1.36 ± 0.03
P_i + maltoheptaose	1.74 ± 0.07	1.61 ± 0.03
P_i + glycogen	1.77 ± 0.03	1.60 ± 0.03
glucose-1-P	1.3–1.69 (varies)	1.3–1.66 (varies)
glucose-1-P + maltoheptaose	1.69 ± 0.06	1.58 ± 0.02
glucose-1-P + glycogen	1.72 ± 0.08	1.59 ± 0.06
glucose-1-P + P_i	1.45 ± 0.04	1.47 ± 0.02
glucose-1,2-P	1.73 ± 0.05	1.69 ± 0.02
glucose-1,2-P + maltoheptaose	1.65 ± 0.06	1.58 ± 0.03
glucose-1,2-P + glycogen	1.80 ± 0.05	1.59 ± 0.02

[a] Additions: 100 mM glucose, P_i, glucose cyclic 1,2-phosphate, PP_i, 10 mM maltoheptaose, and 0.4% glycogen. [b] AMP bound.

Table II: Transient Decay Rate Constants for Analogue-Reconstituted Enzymes

substrate[a]	rate constant ($s^{-1} \times 10^{-5}$) pyridoxal phosphorylase *b*[b]	pyridoxal 5′-fluorophosphate phosphorylase *b*[b]	pyridoxal 5′-pyrophosphate phosphorylase *b*[b]
none	0.93 ± 0.01	1.41 ± 0.01	1.38 ± 0.02
glucose	1.17 ± 0.03	1.30 ± 0.01	1.38 ± 0.03
maltoheptaose	1.12 ± 0.02	1.30 ± 0.01	1.34 ± 0.02
glycogen		1.40 ± 0.02	1.42 ± 0.02
P_i	1.66 ± 0.03	1.87 ± 0.02	1.31 ± 0.02
P_i + glucose	1.46 ± 0.11	1.31 ± 0.01	1.43 ± 0.03
P_i + maltoheptaose	1.58 ± 0.04	1.37 ± 0.03	1.28 ± 0.01
P_i + glycogen	1.53 ± 0.04	1.66 ± 0.02	1.31 ± 0.02
glucose-1-P	1.12 ± 0.01	varies	1.09 ± 0.01
glucose-1-P + maltoheptaose	1.72 ± 0.04	1.39 ± 0.02	1.16 ± 0.02
glucose-1-P + glycogen	1.54 ± 0.05		1.09 ± 0.01
glucose-1-P + P_i + maltoheptaose	1.38 ± 0.03		
glucose-1,2-P		1.68 ± 0.03	1.43 ± 0.01
glucose-1,2-P + maltoheptaose		1.43 ± 0.03	1.43 ± 0.02
glucose-1,2-P + glycogen		1.65 ± 0.02	1.37 ± 0.04
PP_i	1.72 ± 0.08		
PP_i + glucose-1-P	1.32 ± 0.09		
PP_i + maltoheptaose	1.38 ± 0.11		

[a] Additions: 100 mM glucose, P_i, glucose-1-P, glucose cyclic 1,2-phosphate, PP_i, 10 mM maltoheptaose, and 0.4% glycogen. [b] AMP bound.

Table III: Effect of AMP on the Transient Decay Rate for Phosphorylase *b*

substrate[a]	rate constant ($s^{-1} \times 10^{-5}$) no addition	10 mM AMP added
none	1.44 ± 0.01	1.45 ± 0.01
glucose	1.33 ± 0.01	1.31 ± 0.01
P_i	1.51 ± 0.02	2.01 ± 0.03
glucose-1-P	1.32 ± 0.02	1.70 ± 0.04
glucose-1-P + glycogen	1.32 ± 0.02	1.61 ± 0.04

[a] Additions: 100 mM glucose, P_i, glucose-1-P, and 0.4% glycogen.

Discussion

The numerical analysis in this work with its better resolved data proved that the observable decay was more complex than previously thought by Cornish and Ledbetter (1984a). Between the two studies, the results for phosphorylase *b* (1.49 $\times 10^5$ s^{-1}) are in agreement, but some differences with substrates have appeared. The rate of decay for added P_i increased (2.05×10^5 s^{-1}) as before, but the number is slightly

different. Glucose added after P_i decreased the rate to 1.27 $\times 10^5$ s^{-1} as previously observed. A significant difference occurred with the glucose-1-P substrate. This study greatly extended the data to include the rate values for the reactive ternary complex.

In Table I, little change occurred in the numbers with polysaccharide additions to native enzyme. The reduced rate for the glucose molecule underscores a difference between substrate and the inhibitor glucose which forms the T state. Also, we note in Table II that the numbers for pyridoxal-reconstituted enzyme are the same for glucose, maltoheptaose, and glucose-1-P.

The binding of P_i by phosphorylases *a* and *b* and by pyridoxal-reconstituted and pyridoxal 5′-fluorophosphate reconstituted enzymes caused a similar increase in the rate constant. Cornish and Ledbetter (1984a) attributed this change for phosphorylase *b* to the deprotonation of the 5′-HPO_4 group. Because we now find that this increase occurred also with the cofactor analogues, the effects are not simply due to deprotonation but involve other factors as well. Factors which can affect the transient decay rate include the structure of the cofactor molecule, the ionization state of the 5′-PO_4 group, and the protein environment of the cofactor. The first of these expresses itself well in the pyridoxal-reconstituted enzyme. The decay is predictably slower, 0.93 $\times 10^5$ s^{-1} compared to 1.49 $\times 10^5$ s^{-1} for phosphorylase *b*. The slower rate continues through the list of substrates. The rate of 5′-fluorophosphate and 5′-pyrophosphate analogue enzymes was slightly reduced from that of native enzyme. The fact that the rate increases to similar extents on the addition of P_i to cofactor analogue systems which cannot deprotonate requires consideration of the environment of the cofactor as well. Because the transient state is one in which the proton has not returned to the 3-O^- group from the $-NH^+$, the state is a strong dipole, and as such, polar environments will stabilize the state. The following experiment demonstrates this.

The aniline Schiff base of salicylaldehyde exhibits the same type of excited-state proton transfer in a wide variety of solvents. This molecule presents an opportunity to investigate solvent polarity on the rate constant of the 470-nm absorption band. Figure 7 shows a 2 order of magnitude change of the rate constant in going from 3-methylpentane to 2-propanol in which the decay rate is the slower. The plot of log *k* against E_T, an empirical parameter of solvent polarity (Reichardt, 1965), reflects the stabilizing influence of the poar solvents. E_T represents the interaction between solvent and the zwitterionic pyridinium *N*-phenolbetaine molecule. Specifically, it is the energy of the charge transfer transition of the molecule. In shifting the transition band to higher energy, the more polar solvent stabilizes the ground state to a greater degree than it does the less polar excited state of the molecule. This is also the case for the lower state of the transient band of the pyridoxal Schiff bases. On excitation, negative charge transfer from the 3-O^- out to the $-NH^+$ group decreases the polarity.

Hence, in the environment of the cofactor in the enzyme, we must be cognizant of the polar groups affecting the stability of the transient state. Among those are the $-NH^+$ side chains of lysine or arginine which interact with the 5′-PO_4 group and substrate phosphate. Considering that the interactions take place in a protein matrix, any movement of charges about the PLP can determine the transition-state decay rate. The simplest picture to imagine for the addition of P_i, for example, is that the positive side chains orient toward the bound P_i interacting less with the PLP site. This reduction of polarity at the cofactor molecule should cause the transient state to

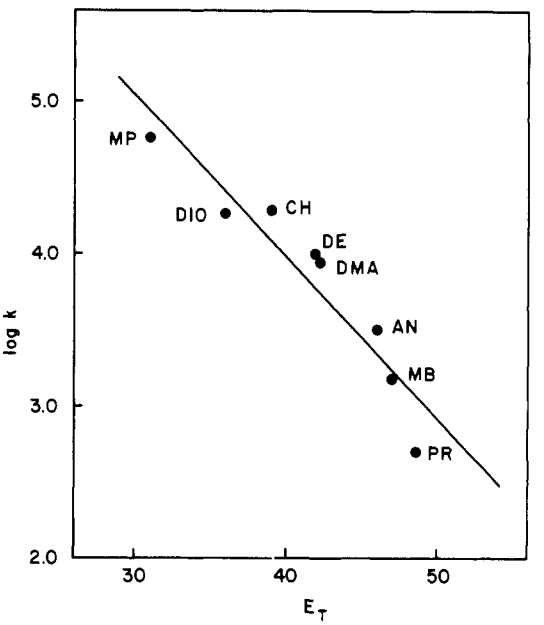

FIGURE 7: Plot of the rate constant of the decay of transient absorbance for salicylideneaniline against E_T (see text) for the solvent. MP, 3-methylpentane; DIO, *p*-dioxane; CH, chloroform; DE, 1,2-dichloroethane; DMA, *N*,*N*′-dimethylacetamide; AN, acetonitrile; MB, 3-methyl-1-butanol; PR, 2-propanol.

decay faster. This movement of positive charge away from the cofactor also causes the 5′-PO_4 to become more negative. The breaking of an ionic bond with a cationic protein residue may have the effect of deprotonation as seen with ^{31}P NMR spectra. The addition of glucose to the P_i complex reverses the rate constant and presumably the movement. In phosphorylase *b*, the rate for P_i plus glucose reflects that of the T state. Cornish and Ledbetter (1984a) also observed this reversal. Alternatively, instead of the isolated movement of side chains affecting these changes, the movement of regions or domains as suggested by Madsen and Withers (1984) may well provide the environmental change.

When first added to the enzyme, glucose-1-P yields a rate constant of 1.3 $\times 10^5$ s^{-1}, similar to that for glucose. This observation indicates that glucose and glucose-1-P binds at the same site. Sprang et al. (1982) conclude from X-ray analysis of phosphorylase *a* that binding occurs at the same site. Madsen et al. (1978) also suggest that the phosphate acts as a conformational trigger for the R state. We do observe that the rate for native enzyme increases with time to about 1.7 $\times 10^5$ s^{-1} for glucose-1-P and not for glucose. The enzyme achieves this upper limit for glucose-1-P as shown in Table I within 30 min. With added polysaccharide, the ternary complex achieves this upper limit quicker, although the number for phosphorylase *b* is slightly lower. We strongly suspect that the low number of 1.3 $\times 10^5$ s^{-1} for glucose represents the known T state and that the change to higher numbers for glucose-1-P additions reflects a change to the R state.

The addition of polysaccharide to glucose-1-P to form the reactive ternary complex further changes the rate constant. The new constant is the same as that for the addition of polysaccharide to P_i (1.6 $\times 10^5$ s^{-1}). The observation strongly suggests that the resulting conformations are basically the same—the same activated complex. The numbers are between those for enzyme and for enzyme plus P_i but closer to the enzyme's rate constant. Our interpretation requires that the P_i moves within the active site to a position closer to the 5′-PO_4 or occupies a position coincident with that for the phosphate of glucose-1-P.

With the competitive inhibitor glucose cyclic 1,2-phosphate, the rate constants agreed with the 1.7×10^5 s^{-1} for glucose-1-P but without any change with time. With the addition of polysaccharide, it is highly remarkable for the numbers for its ternary complexes (1.6×10^5 s^{-1}) to agree so well with those for P_i and glucose-1-P ternary complexes. We believe this means that the phosphates of the substrate and the cofactor are in the same relative positions in the protein matrix of the different ternary complexes. These rate constants for this protein conformation must surely represent the transition-state conformation of the R state. The rate constants for phosphorylase *a* are 0.1×10^5 s^{-1} unit higher and contain more error, but show the same effect for the ternary complexes.

The rate constants of Table III demonstrate quite nicely that the observable depends on the active-site protein conformations. Without bound AMP, P_i did not exert its effect at the active site. Only after addition of AMP did it do so. The same was true for glucose-1-P. In fact, without AMP, glucose-1-P bound like glucose. On addition of AMP, the rate constant increased to 1.7×10^5 s^{-1}, which is equal to that observed in Table I. With the addition of glycogen, the AMP shifted the constant to 1.6×10^5 s^{-1}, equivalent to that in Table I for the ternary complexes.

The rate constants of Table II also appear to show an active ternary complex for the pyridoxal-reconstituted enzyme. This enzyme reportedly has some activity in the presence of a noncovalently bound anion activator (Parrish et al., 1977) which occupies the phosphate binding site of the cofactor. Pyrophosphate inhibits the reaction apparently by occupying this phosphate site and the glucose-1-P site simultaneously. In our study, the increase in the rate constant for P_i bound to the enzyme (1.66×10^5 s^{-1} compared to 0.93×10^5 s^{-1} for the enzyme) indicates that P_i occupies its substrate binding site. It could also be binding at the cofactor phosphate site, but the rate constant indicates binding at the phosphate site. The addition of polysaccharide had only a small decreasing effect. Glucose-1-P had the same small effect as that of polysaccharide or glucose. Glucose-1-P and polysaccharide added together to the enzyme yielded a number indicating binding at the phosphate site. With P_i added to the glucose-1-P and polysaccharide, after a period of 30 min to 1 h the constant changed from 1.53×10^5 to 1.38×10^5 s^{-1}. This indicated movement of phosphate at the active site toward the ternary complex. This could indicate an R-state configuration for the pyridoxal-reconstituted enzyme. With added pyrophosphate, the rate constant of 1.72×10^5 s^{-1} indicated binding at the substrate phosphate site. Only when the enzyme bound glucose-1-P or maltoheptaose with PP_i did the value decrease, again indicating binding nearer the cofactor phosphate site and further from the substrate phosphate site. The regression error for the PP_i additions was higher, which makes a conclusion more tenuous. However, the 1.38×10^5 s^{-1} observed for the ternary complex with P_i and for the inhibitor, PP_i, plus polysaccharide is striking, making more plausible the idea that the phosphates of the R state are near.

The substitutions on the 5′-PO_4, i.e., F and PO_4, which form the cofactor analogues had a small effect on the decay rate (1.4×10^5 s^{-1}) of enzyme alone, in particular. In the substitution of a second phosphate group, the inductive effect changes only slightly. What is notable is the lack of a large observable effect on the protein conformation by the presence of the second phosphate of the pyrophosphate group. One might expect that if an electrophilic attack by a constrained 5′-PO_4 on an adjacent PO_4 occurred within a short distance, the 5′-pyrophosphate cofactor might elicit the reactive protein

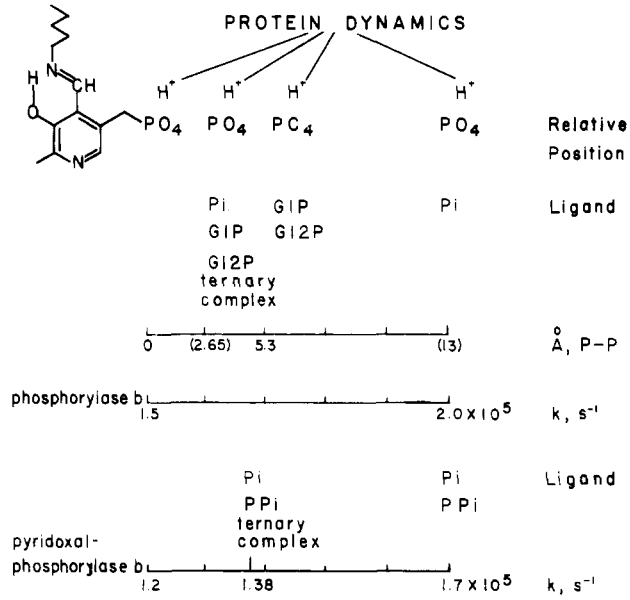

FIGURE 8: Movements of the H^+ charges represent different protein conformations which confer degrees of polarity at the cofactor. The X-ray data for glucose cyclic 1,2-phosphate in phosphorylase *b* provided the basis for the distances in angstroms between phosphates. Extrapolated distances based on the rate constants occur in parentheses.

conformation. Certainly this argument was put forth in the use of pyridoxal 5′-pyrophosphate glucose. We observed a small change in a direction which itself may be taken to mean that the second phosphate is in the wrong position for the reactive ternary complex shown by phosphorylases *a* and *b*. Also quite noteworthy, the rate constants for the 5′-pyrophosphate enzyme analogue do not change significantly with substrates. The possible exception is with glucose-1-P addition. This lack of change indicates that the 5′-pyrophosphate group locks in a particular conformation not allowing any movement of the protein positive charge away from the cofactor. None of the rate constants, particularly those of glycogen and maltoheptaose, indicate the reactive configuration of phosphorylase *b*. Substitution of fluorine allows conformational changes in all substrates but maltoheptaose in the ternary complex. This observation demonstrates that while the 5′-PO_3F charge is different, the substrate phosphate position in the protein matrix is a key requirement for catalysis.

This paper offers largely three contributions: (1) the observations present a new perspective upon protein conformations about the cofactor active site of polar residues which probably affect not only the deprotonation of the 5′-PO_4 observed with ^{31}P NMR but clearly also the mechanism for catalysis; (2) the observations provide a vista of the phosphate–residue interactions as the various substrates bind and of an active transition state approached from either direction of the phosphorylase reaction; and (3) the observations of the 5′-pyrophosphate cofactor as a test for an electrophilic attack by a constrained dianionic 5′-PO_4 do not represent an active protein conformation.

Schematically in Figure 8, we wish to emphasize a relationship between protein charge movement and substrate phosphate positions. In accordance with such, we recognize an active ternary complex in which the phosphates of cofactor and substrate (glucose-1-P or P_i) move into close proximity for reaction. Madsen and Withers (1984) reported that the most effective inhibition by alkane diphosphonates occurs with methylene, in which case the P–P separation is 3 Å. McLaughlin et al. (1984) demonstrated with X-ray diffraction studies that during the formation of heptulose 2-phosphate by

glycogen phosphorylase *b* the P–P distance is only 4.5 Å. The P–P separation for pyrophosphate is 2.9 Å, but our observations on the enzyme analogue do not support this distance. The calculated P–P separation for hydrogen-bonded phosphates is 3.9–4.8 Å, a range probably more realistic.

The extrapolated value of 13 Å for P_i is interesting. P_i with AMP has a significant effect on increasing the rate constant and on decreasing the amplitude of the slower decays. Where exactly it binds for these effects is a puzzle. It does compete with the effector site 30 Å away from the pyridoxal-5′-P (Sygusch et al., 1977), but the rate constant for P_i without AMP does not support any conformational change at the active site. Instead, rate constant data suggest that P_i with AMP binds at the active site but not close to the 5′-PO_4. A value as large as 13 Å is not unrealistic for a P–P distance at the active site, considering that the molecular crevice leading to the active site is on the order of 15 Å deep (Johnson et al., 1980) and contains several positively charged groups within 10 Å of the glucose binding site (Arg-568, His-570, Lys-573) (Fletterick & Madsen, 1980; Madsen & Withers, 1984; Sansom et al., 1984).

In the activated ternary state, we do not observe a gross proton exchange dependent on the P_i or glucose-1-P substrates. We do not see strong localization at the cofactor phosphate of protein positive charges, which should produce slower decay rates. Instead, the increase in the decay rate constant shows the cofactor in the ternary complex in a less polar environment. With the increase in the rate constant, we depict in Figure 8 a protein positive charge moving from the 5′-PO_4 to substrate phosphate. The decrease in the charged environment will increase the pK_a of the 5′-PO_4 group. Perhaps this ability to adjust in acidity is sufficient to maintain an electron pull through a hydrogen-bonded substrate phosphate for cleavage of the latter or, conversely, for activation of P_i. For catalysis, the group covalently linked to 5′-CH_2OH must be protonatable in the pH range of phosphorylase activity (Klein et al., 1984). The concurrent increase of protein positive charge at the substrate phosphate would promote the polarization.

Added in Proof

More recently, a Fourier transform analysis requiring no input parameters found for the decay curve for phosphorylase *b* four exponentials at 873 000, 150 000, 30 000, and 7000 s^{-1}.

Acknowledgments

We are grateful to Timothy Cornish for his help in obtaining the data of Figure 7.

Registry No. P_i, 14265-44-2; PP_i, 14000-31-8; G1P, 59-56-3; G12P, 64161-84-8; AMP, 61-19-8; D-glucose, 50-99-7; maltoheptaose, 34620-78-5; glucogen, 9005-79-2; phosphorylase *a*, 9032-10-4; phosphorylase *b*, 9012-69-5; glycogen phosphorylase, 9035-74-9.

References

Cornish, T. J., & Ledbetter, J. W. (1984a) *Eur. J. Biochem. 143*, 63–67.

Cornish, T. J., & Ledbetter, J. W. (1984b) *IEEE J. Quantum Electron. QE-20*, 1375–1379.

Cornish, T. J., & Ledbetter, J. W. (1985) *Photochem. Photobiol. 41*, 15–19.

Dreyfus, M., Vandenbunder, B., & Buc, M. (1980) *Biochemistry 19*, 3634–3642.

Fischer, E. H., & Krebs, E. G. (1958) *J. Biol. Chem. 231*, 65–83.

Fletterick, R. J., & Madsen, N. B. (1980) *Annu. Rev. Biochem. 49*, 31–61.

Johnson, L. N., Jenkins, J. A., Wilson, K. S., Stura, E. A., & Zanotti, G (1980) *J. Mol. Biol. 140*, 565–580.

Klein, H. W., Palm, D., & Helmreich, E. J. M. (1982) *Biochemistry 21*, 6675–6684.

Klein, H. W., Im, M. J., Palm, D., & Helmreich, E. J. M. (1984) *Biochemistry 23*, 5853–5861.

Krebs, E. G., Love, D. S., Bratvold, G. E., Traysen, K. A., Meyer, W. L., & Fischer, E. H. (1964) *Biochemistry 3*, 1022–1033.

Ledbetter, J. W., Askins, H. W., & Hartman, R. S. (1979) *J. Am. Chem. Soc. 101*, 4284–4289.

Madsen, N. B., & Withers, S. G. (1984) in *Chemical and Biological Aspects of Vitamin B6 Catalysis: Part A*, pp 117–126, Alan R. Liss, New York.

Madsen, N. B., Kasvinsky, P. J., & Fletterick, R. J. (1978) *J. Biol. Chem. 253*, 9097–9101.

McLaughlin, P. J., Stuart, D. I., Klein, H. W., Oikonomakos, N. G., & Johnson, L. N. (1984) *Biochemistry 23*, 5862–5873.

Parrish, R. F., Uhing, R. J., & Graves, D. J. (1977) *Biochemistry 16*, 4824–4831.

Reichardt, C. (1965) *Angew. Chem. 4*, 29–40.

Sansom, M. S. P., Babu, Y. S., Hajdu, J., Stuart, D. I., Stura, E. A., & Johnson, L. N. (1984) in *Chemical and Biological Aspects of Vitamin B6 Catalysis: Part A*, pp 127–146, Alan R. Liss, New York.

Shaltiel, S., Hedrick, J. L., & Fischer, E. H. (1966) *Biochemistry 5*, 2108–2116.

Shimomura, S., & Fukui, T. (1978) *Biochemistry 17*, 5359–5367.

Sprang, S. R., Goldsmith, E. J., Fletterick, R. J., Withers, S. G., & Madsen, N. B. (1982) *Biochemistry 21*, 5364–5371.

Sygusch, J., Madsen, N. B., Kasvinsky, P. J., & Fletterick, R. J. (1977) *Proc. Natl. Acad. Sci. U.S.A. 74*, 4757–4761.

Takagi, M., Fukui, T., & Shimomura, S. (1982) *Proc. Natl. Acad. Sci. U.S.A. 79*, 3716.

Walters, L. S., Cornish, T. J., Askins, H. W., & Ledbetter, J. W. (1982) *Anal. Biochem. 127*, 361–367.

Weber, I. T., Johnson, L. N., Wilson, K. S., Keats, D. G. R., Wild, D. L., & Jenkins, J. A. (1978) *Nature (London) 274*, 433–437.

Withers, S. G., Madsen, N. B., Sykes, B. D., Takagi, M., Shimonura, S., & Fukui, T. (1981a) *J. Biol. Chem. 256*, 10759–10762.

Withers, S. G., Madsen, N. B., & Sykes, B. D. (1981b) *Biochemistry 20*, 1748–1756.

Withers, S. G., Madsen, N. B., Sprang, R., & Fletterick, R. J. (1982) *Biochemistry 21*, 5372–5382.

Wittmann, R. (1962) *Angew. Chem., Int. Ed. Engl. 1*, 213.